A Simulation Approach to Optimizing Performance of Equipment for Thermostimulation of Muscle Tissue using COMSOL Multiphysics

J. Kocbach[1], K. Folgerø[1], L. Mohn[2], and O. Brix[1]
[1]Christian Michelsen Research AS, P.O.Box 6031, NO-5892, Bergen, Norway
[2]The Luzmon UK, 45 Phillimore Walk.London W8 7RZ. England – UK
jan@cmr.no

Keywords: Thermostimulation, CAD, Multiphysics, Microwave, Heat therapy, Electrical stimulation, Infrared

Abstract: A multiphysics simulation approach is used in order to analyse and optimize performance of thermostimulation equipment. The temperature distribution and electric field distribution within the body tissue is simulated for varying body composition, for varying design parameters of the thermostimulation equipment and for different heating methods. Based on these simulations, information is gained regarding design choices for thermostimulation equipment, and relative effectiveness of thermostimulation equipment for patients with different body composition. The finite element package COMSOL Multiphysics is used for the simulations.

1 INTRODUCTION

Thermostimulation is a combination therapy which involves the use of heat therapy and electrical stimulation simultaneously. With thermostimulation, the healing benefits of heat are provided along with the strengthening, toning, pain relieving and healing benefits of electrical stimulation. Moreover, the application of heat has been found effective in that it allows the patient to tolerate higher currents in the electrical stimulation process. This yields higher electric field strengths, greater depths of penetration and therefore more positive results than could be achieved with electrical stimulation without heat.

The challenge is to design thermostimulation equipment which gives sufficient high temperature and sufficient electric field strength within all of the muscle tissue to be treated. Both the temperature and the electric field distribution will in the general case be non-uniform, and vary with layout and type of heating and stimulation equipment, body composition, muscle type and several other parameters. It is possible to investigate how these parameters influence on the thermostimulation effect by using multiphysics simulations. Simulations can help understand how the body composition, in particular fat layer thickness, influences on the maximum temperature achievable in the muscles and the amount of muscle stimulation. Simulations can also be applied to compare conventional heating using heat pads with alternative heating methods like infrared heating or microwave heating – both regarding maximum temperature and heating time.

A number of works have been published on computer simulations related to different aspect of electric stimulation and heating of tissue. Examples include the work of Kuhn and Keller (2005) that used a 3D transient model to study how the capacitive effects influence the nerve and muscle activation. Filipovicet al (2011) also developed a transient 3D finite element model, and fitted the tissue properties of the model to match the response measured on a volunteer, whereas Reichel et al. (1999) studied excitation of denervated muscle fibres caused by surface electrodes. Fiala et al (1999) developed a whole-body computer model predicting the human thermal responses to environmental changes. More local heating effect was studied by Drizdal et al. (2010) who developed a 3D model in COMSOL Multiphysics and showed that the temperature

dependency of the blood perfusion should be included in order to model the temperature distribution accurately.

The present work illustrates how a multiphysics simulation approach can be used to calculate the temperature and electric field distribution within the body tissue when applying the thermostimulation equipment, specifically in the muscle tissue. It also discusses how such simulations can be used in order to optimize performance of thermostimulation equipment by modifying the layout of the heat pads and stimulation electrodes, and by comparing different heating methods. The finite element package COMSOL Multiphysics is used for the simulations.

2 BACKGROUND

2.1 Heating of biological tissue

Heat can be delivered to the muscle tissue in several ways, for instance by placing the patient in a heated environment, by applying a heat element at the skin surface, or by using radiated electromagnetic or ultrasonic energy. Heat transfer can occur through conduction, convection, or radiation. Conduction is transfer of heat energy between objects in physical contact, conduction is transfer of energy between an object and its environment due to fluid motion, and radiation heating is transfer of energy through emission or absorption of radiated energy. Transpiration from the skin surface also takes part in the overall heat transfer, but is not considered further as we are most interested in heat transfer into the body tissues.

Hyperthermia is defined as raising the temperature of a part of or the whole body above normal for a period of time (Habash 2006). Hyperthermia is a well-established cancer treatment method – often used in combination with radiotherapy or chemotherapy. Hyperthermia is also applied for management of muscle and tendor injuries (Giombini 2007), taking advantage of the regional increase in blood flow., The blood perfusion increases by about 15 times when the tissue temperature raises from 36°C to 45°C (Giombini 2007), and effective clinical responses have been found when the temperature at the injured site are increased to therapeutic temperatures of 41-45°C. However, exposure above normal physiologic ranges (i.e. above 42 °C) can result in measurable irreversible changes in tissue structure (Kreith & Goswami 2005), as e.g. cell death or tissue alterations like skin burns. Irreversible thermal damage is found to be exponentially dependent on temperature and linearly dependent on time of exposure, and for a temperature of 44 °C, the threshold time for a second degree burn was found to around 7 hours in experiments reported by Kreith & Goswami (2005). For the study considered in this paper, the maximum heat applied at the skin is therefore set to 42 °C.

Heat transport mechanisms in biological tissues can be modelled by the "bioheat equation" originally described by Pennes (Pennes 1948)

$$\rho C_p \frac{\partial T}{\partial t} + \nabla \cdot \left(-k \nabla T\right) = \rho_b C_b \omega_b \left(T_b - T\right) + Q_{met} \qquad (1)$$

where ρ is the tissue density [kg/m^3], C_p is the tissue heat capacity [J/kgK], T is the tissue temperature [K], k is the tissue thermal conductivity [W/mK], ρ_b is the density of blood [kg/m3] , C_b is the heat capacity of blood [J/kgK], ω_b is the tissue blood perfusion rate [1/s], T_b is the arterial blood temperature [K], and Q_{met} is the metabolic heat generation [W/m^3].

The bioheat equation consists of 4 terms representing heat storage, heat conduction, heat convection (blood perfusion) and metabolism. The metabolic heat generation is the sum of the basal metabolic rate and local autonomic thermoregulation (exercising and shivering) (Fiala et al. 1999).

There are some limitations related to the fundamental assumptions of the Pennes model (Kreith & Goswami 2005), and several extensions and modifications of the Pennes model have been suggested. For example, Bronzino (2000) claims that in order to get realistic results, ω_b and T_b should be taken as adjustable parameters determined by e.g. curvefitting, and not literally as blood perfusion rate and arterial blood temperature. However, the model has nevertheless proved to be in good agreement with experimental findings and is the primary choice for heat transport analysis (Kreith & Goswami 2005), and thus the Pennes model is used for the simulations in the current work.

Several different approaches to heat the muscle tissue are considered in this paper. The first of these approaches is to use heat pads which transfer heat from the external pad to the skin through conduction. The heat is then transferred to deeper tissues also through conduction, while convection between blood and the vessel walls oppose the heating. Thus, the heat conductivity and blood perfusion are the most important parameters to know in order to model heating by external heat elements. Depending on the fat layer thickness, the heating effect of the muscles may be quite small, as fat has a low thermal conductivity.

A second approach considered is using infrared (IR) energy. This occurs through absorption of radiation by the skin, and the heat is then transferred to deeper tissues by thermal conduction. Skin is not transparent to IR radiation, and the penetration depth is in the order of mm (ICNIRP 2006, Bjordal 2001). Thus the effect of heating using IR energy is expected to be only marginally better than traditional heat pads.

A third approach is heating through microwave and radio frequencies (RF). Radiation at microwave and radio frequencies can penetrate the relatively thin skin layer and reach deeper into the tissue before being absorbed. The penetration depth increases with decreasing frequency, and is typically in the range of cms for microwaves (compared to mms for IR) – depending on the dielectric properties of the tissue. Fat is quite transparent to RF and microwaves, whereas the skin layer is thin and therefore does not absorb much RF/microwave energy. Thus, most of the RF/microwave energy is absorbed by the muscles. The heat will then be distributed from the muscles to other tissues through heat conduction. This direct heating of the muscles will take place much faster than the indirect muscle heating obtained with heat pads and infrared heating.

2.2 Electrical muscle stimulation

In thermostimulation, electrical stimulation is usually done by applying a current at the surface of the body, using a set of electrodes in contact with the skin. This current leads to an electric field being set up in the underlying tissue. This leads to stimulation of nerves and/or muscles when the electric field at the nerve/muscle cell location inside the muscles is above a certain threshold. The stimulation gives muscle contractions, which increases the muscle blood flow and muscle strength.

The electric field induces muscle contractions in two different ways. The first method is stimulation of motor neurons (nerve cells), which then excite the muscle fibers by chemical transmission. A single motor neuron innervates many muscle fibers. A motor neuron and the muscle fibers it innervates are called a motor unit. All the muscle fibers of a motor unit contract together when they are stimulated by the motor neuron, and develop force. The second way is direct stimulation of muscle fibers (muscle cells). Muscle fibers are long cylindrical cells 50 to 100 um in diameter, sometimes running the entire length of a muscle. The muscle fibers are grouped in bundles surrounded by connective tissue. The contraction occurs due to the current/electric field variations set up over the individual muscle fibers by the stimulation electrodes. Usually only denervated muscle fibers will be stimulated through direct stimulation of muscle fibers (Nelson et al. 1999) due to the fact that the stimulation threshold is 2-3 times higher for direct muscle stimulation compared to nerve stimulation (Mortimer et al. 2004).

The stimulation threshold is the threshold for which the first muscle cells are stimulated – typically the ones which lay at locations for which the electric field/current in the tissue is at its maximum. When increasing the current applied over the electrodes further towards the maximum pain tolerance threshold (see Figure 1), more and more muscle cells/muscle units are stimulated as the electric field and current is increased deeper into the

muscle and along all the length of the muscle. Thus it is the electric field and current in the muscle which is the important factor rather than the current applied at the skin (which is usually given in published work).

The electric field in the muscle varies significantly with a number of factors, like e.g. electrode size, electrode spacing, thickness of tissue layers (especially the skin layer), skin conductivity and pulse length. By varying factors like electrode size, electrode spacing and pulse length, it is possible to influence the distribution of the electric field in the tissue, and thus also the stimulation. It is difficult to perform in vivo measurement of the electric fields distribution, but the influence can be investigated using multiphysics simulations.

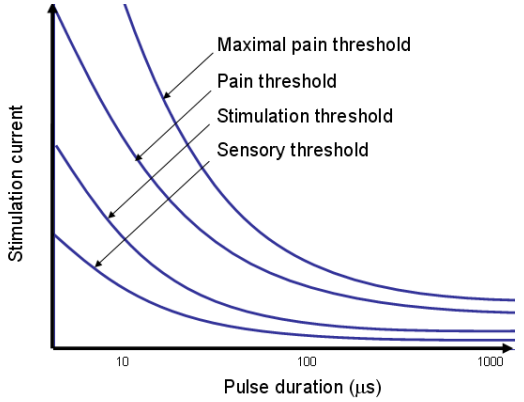

Figure 1. Relationship between pulse duration and stimulation current based on data from Nelson et al. (1999). The lowest curve represents the sensory threshold, the second curve the stimulation threshold, the third curve the pain threshold and the fourth curve the maximal pain threshold.

3 MODELLING

A multiphysics approach has been used to study thermostimulation in the current work. All simulations have been carried out using the Finite Element (FE) tool COMSOL Multiphysics, which is a module based FE software widely used in physics and engineering. The AC/DC and RF modules have been used for the electromagnetic (EM) simulations and the heat module has been applied for the heat simulations. For the combined heat/EM simulations, the different modules have been applied simultaneously in a multiphysics model.

The body tissue has been modelled as a layered structure, consisting of a bone layer, a muscle layer, a fat layer and a skin layer. The simulation models are described in detail in the subsections below. Convergence tests with varying meshes have been done in order to ensure fully converged solutions for all models (not shown). Three different types of simulations have been considered; steady state simulations, frequency domain simulations and transient time domain simulations.

Biological tissue properties found in the literature vary significantly between different sources. Also, it must be noted that the blood perfusion rate and metabolic heat generation depends strongly on the metabolic and thermoregulatory needs of the tissue, and the bioheat equation has fundamental limitations. In addition the tissue layers are assumed to be isotropic, i.e. the anisotropy in the tissue is not included. Kuhn & Keller (2005) showed that the significant differences in tissue parameters for muscles in the longitudinal direction compared to the transversal direction have a notable influence on the simulation results. Thus the focus for the simulations has been to get a qualitative understanding of the processes involved, and the outcome of the simulations must therefore be interpreted with great care. Material parameters applied in the current work are described in section 3.4 below.

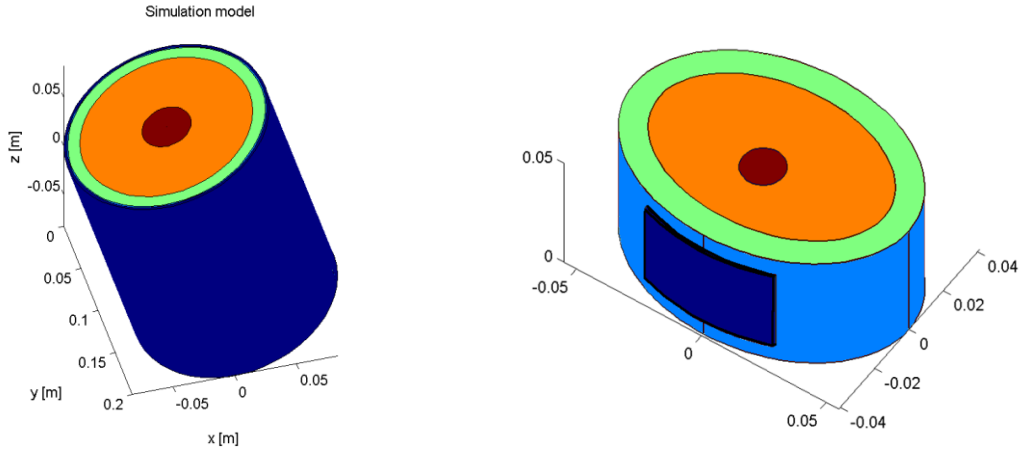

(a) (b)

Figure 2. Simulation models for conventional heating of tissue using heat pads (a) Axisymmetric model. (b) 3D model.

3.1 Conventional heating models

The axisymmetric model for conventional heating (i.e. using heat pads) has been built up using uniform layers [see Figure 2(a)]. The layers as seen from the center of the model are bone (dark red), muscle (orange), fat (green) and skin (light blue, too thin to be properly identified in the axisymmetric model). Outside the skin layer there is a heat pad structure (dark blue), consisting of a silicon rubber layer and a heat wire layer.

The model has been built up to represent a part of a typical thigh in the human body, but results are also applicable to other body parts. The length of the model was set to 200 mm, the radius of the bone to 20 mm, muscle layer thickness to 50 mm, the fat layer thickness was varied between 1 mm and 100 mm (nominal value is 10 mm) and the skin layer thickness was set to 1 mm. The thickness of the silicon rubber layer was set to 2 mm and the thickness of the thin heat wire layer was set to 0.5 mm. Tissue parameters were set according to the parameters defined in Table 1.

Heat wires have been simulated by varying the electrical conductivity in the heat wire layer using a step function. An electric potential was applied over the heat wire layer ($+V_{pad}$ at the upper end of the model, ground at the lower end of the model). This resulted in heat being generated in the parts of the heat wire layer for which the electrical resistance is high, i.e. in the heat wires. The electric potential V_{pad} was adjusted using an iterative process in order to get a maximum temperature of 42 ºC at the parts of the heat pad which are in contact with the skin. For each iteration in the iterative process, two simulations were made. First an electromagnetic simulation in which the electric potential distribution, electric field distribution and electromagnetic losses in the heat pad were calculated. This was followed by a heat simulation in which the heat distribution in the tissue and the heat pad was calculated based on the heat generated by the electromagnetic losses in the heat wires.

The electrical conductivity in the heat wire layer was varied according to the formula

$$y = \sigma_{resistive} + \frac{\sigma_{metal}}{2}\left\{ sgn\left[\cos\left(2\pi N \frac{z}{l_{model}}\right)\right] + 1\right\} \quad (2)$$

where l_{model} is the length of the model, N is the number of heat wires to be applied along the length of the model, σ_{metal} is the electrical conductivity of the part of the heat pad in which no heat is to be generated (heat wire spacing) and $\sigma_{resistive}$ is the electrical conductivity of the part of the heat wire layer in which heat is to be

generated (heat wires). See an example of electrical conductivity distribution in the heat wire layer in Figure 3. Some simulations are also made with an even heat distribution of 42 ºC over all of the skin surface.

A full 3D model for conventional heating has also been built up [see Figure 2(b)]. The 3D model is also a layered model, but the geometry of each layer can be shaped individually instead of axisymmetric. Also, the heat pads in the 3D model only cover part of the skin.

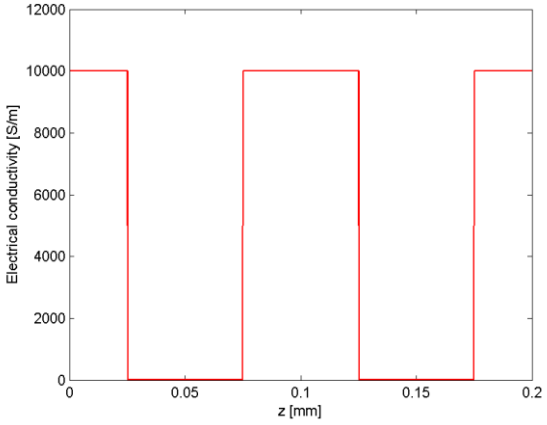

Figure 3. Example of variation in electrical conductivity as a function of position (z) in the heat wire layer for the case N=2. The z-dimension is defined in Figure 2(a)

3.2 Infrared (IR) and microwave heating models

An axisymmetric models for IR heating have been built up analogously to the axisymmetric conventional heating model shown in Figure 2(a), except no heat pad layer was included. The heating of the tissue by IR energy was approximated by a heat generation term Q which is calculated based on a one-dimensional energy propagating model, and applied at the outer surface of the skin. As the wave travels in the tissue, the energy is dissipated as heat in the tissue. This dissipated energy was included in the Finite Element implementation through the heat generation term Q. Heat conduction has been handled in the heat module in COMSOL Multiphysics in the same manner as for the conventional heating model.

The decay of IR energy into a tissue can be approximated by an exponential decay given by Datta & Rakesh (2009)

$$Q = Q_0 e^{-\frac{z}{\delta}}, \tag{3}$$

where Q_0 is the volumetric heating at the surface and δ is the penetration depth of the IR energy at the particular wavelength. The penetration depth is defined as the depth were the field power is reduced by 1/e, and can be found as

$$\delta = \frac{1}{\alpha}, \tag{4}$$

where α is the attenuation coefficient of the material. The attenuation coefficient varies as a function of wavelength and also between different tissues. Measured values of the IR power attenuation coefficient can be found in tabulated data for some types of tissues (see Table 1).

The volumetric heating Q can be expressed through the energy flux I_0 by (Datta & Rakesh 2009)

$$Q = \alpha I. \tag{5}$$

In the Finite Element implementation, Q is calculated for any position z in the layered model by Eq. (5) using different power attenuation coefficients for the different layers in the model. The energy flux I_0 at the skin is adjusted using an iterative process in order to get a maximum temperature of 42 ºC in the tissue.

A full 3D multiphysics model has been set up to study the microwave heating case (see Figure 4) following the work of Drizdal et al. (2010). The model consists of a waveguide (dark red) coupled to a microwave horn (light red) designed to operate at 434 MHz. Both waveguide and horn are filled with deionized water. The waveguide is excited by a TE_{10} mode at 434 MHz. Between the horn and the skin, a water bolus (yellow) with circulating deionized water is included. The temperature of the water can be controlled in order to give a cooling effect on the skin. The skin (dark blue) has thickness 2 mm, fat layer (middle blue) has thickness 10 mm, muscle (cyan) has thickness 108 mm. The area under the aperture is 300 mm x 300 mm. Tissue properties are given in Table 1, and further details about the simulation model are given in (Drizdal et al. 2010).

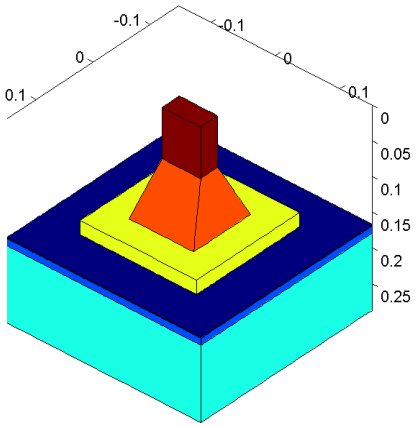

Figure 4. 3D model for microwave heating.

3.3 Electric stimulation models

For the electric stimulation case, a 3D layered simulation model has been set up [see Figure 5 (a)]. From the bottom and up the layers are given as a 10 mm bone layer, a 30 mm muscle layer, a 5 mm fat layer, a 1.5 mm skin layer and a 1 mm stimulation pad layer. In some of the simulations a 1 mm gel layer is included between the skin layer and the stimulation pad layer. The stimulation layer contains two excitation electrodes. For the given case, the electrode length is 190 mm, electrode width is 50 mm and electrode spacing is 50 mm.

A modification to the model was made in which a high conductivity wire was added under each of the electrodes to ensure better distribution of current and potential throughout the length of the electrode. A second modification to the model was to include a strip between the electrodes which can either contain electrically conductive gel, or contain air. Both modifications to the model are indicated in Figure 5 (b).

For analysis purposes, the electric field was calculated along two different lines [cf. illustration in Figure 5 (b)]. Line A is in parallel to the electrodes, positioned in the middle of the gap between the electrodes, 1 mm below the fat/muscle interface. Line B is perpendicular to the electrodes, positioned at 1/4 of the electrode length.

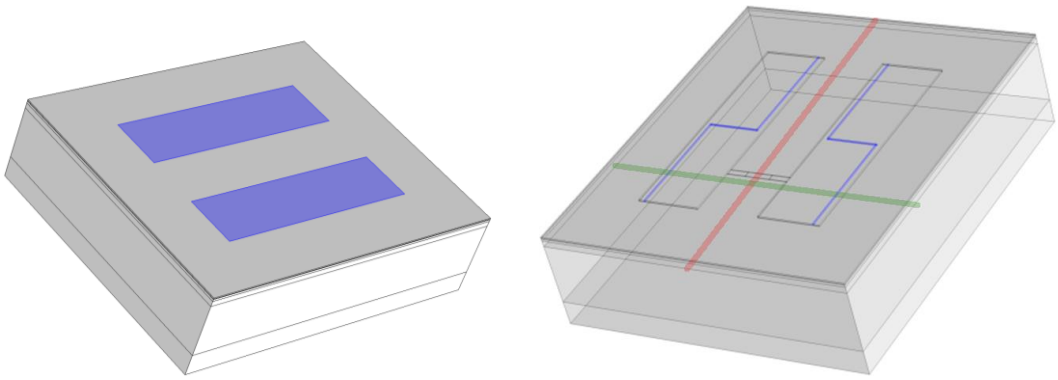

Figure 5. (a) 3D layered simulation model for the stimulation case. The layers from the bottom and up are bone layer, muscle layer, fat layer, skin layer, gel layer and stimulation pad layer. The electrodes are shown as blue solid surfaces. (b) As (a), but with high conductivity wires placed on the electrodes, and with a strip between the electrodes which is used for gel leakage simulations. The wires are shown as blue lines. Also shown are lines along which the electric field is calculated and shown in the analysis part of the present report are shown in red (Line A) and green (Line B).

3.4 Material parameters

The biological tissue properties found from literature vary significantly between different sources, and thus it is not straight-forward to choose which values to use in simulations of thermostimulation problems. The variation of tissue parameters reported by different authors may in some cases lead to significant changes in the simulation results.

In addition, the values given in literature for metabolic heat generation and blood perfusion rate are typically basal values for a person at rest. Furthermore, most papers found in literature treat the material parameters as constants with regard to temperature. However, some papers have been found that include the temperature dependency of e.g. ρ, ω_b and k in simulations [see discussion in (Mohammed & Verhey 2005), (Drizdal et al. 2010)]. Taken into account that the bioheat equation also has fundamental limitations and that the blood perfusion rate and metabolic heat generation depends strongly on the metabolic and thermoregulatory needs of the tissue, the quantitative outcome of the simulations must be interpreted with great care.

A set of properties for biological tissue have been chosen for simulations presented in this report based on comparing parameters from different sources and doing sensitivity analysis (not shown). Thermal and electrical properties of the biological tissues are shown in Table 1, whereas properties for the pad materials are shown in Table 2. Temperature dependency of tissue parameters has not been taken into account in the simulations.

Some of the tissue parameters vary significantly with frequency, thus effectively being a function of the stimulation pulse width. The pulse widths for the available programs usually vary from 100 μs to 500 μs, giving an effective frequency for the pulses of between 2 kHz and 10 kHz. In the simulations in this work a frequency of 10 kHz is used.

There are many different conductive gels available on the market. In (Ward 1984) the conductivity for a number of gels was measured, and conductivities varying from around 0.11 S/m to 6.2 S/m were found. In the current simulations a conductivity of 6.2 S/m is used for the gel in all simulations except for one simulation series. This value should be representative for a good conductive gel, having conductivity somewhat better than seawater.

Table 1. Properties of biological tissues used in the present work from *Carrara (2010), †Duck (1990), ‡Drizdal et al. (2010) and §Fiala et al. (1999).

		Blood	Bone	Fat	Muscle	Skin
Thermal conductivity†	[W/mK]	0.492	0.35	0.25	0.5	0.32
Spesific Heat†	[kJ/kg°C]	3.8	1.3	3.1	3.72	3.45
Density†	[kg/m^3]	1050	1990	928	1041	1100
Blood perfusion rate§	[m^3/s/m^3]	-	0	$0.0036 \cdot 10^{-3}$	$0.538 \cdot 10^{-3}$	$1.05 \cdot 10^{-3}$
Basal metabolic heat rate§	[W/m^3]	-	0	58	684	368
Conductivity* 10 kHz	[S/m]		0.020	0.024	0.341	0.003
Conductivity 434 MHz	[S/m]		0.022†	0.042‡	0.8‡	0.68‡
Rel. Permittivity* 10 kHz			$0.5 \cdot 10^3$	10^3	$25 \cdot 10^3$	$29 \cdot 10^3$
Rel permittivity 434MHz			90†	5.6‡	57‡	49‡
Optical attenuation coefficient**				340 (λ=630 mm)	370 (λ=800 mm)	1000 (λ=1230 mm)

Table 2 Properties of pad materials used in the present work from *Watlow (2010), †Primasil (2010), ‡Matweb (2010) and §Ward (1984).

Material	**Conductivity [S/m]**	**Rel. Permittivity**	**Thermal conductivity (W/mK)**	**Spesific Heat (kJ/kg°C)**	**Density (kg/m^3)**
Stimulation, electrodes (conducting silicon rubber)	40†	7†	0.216*	1.884*	1250*
Stimulation, isolating layer .	1.6e-15‡	7‡	0.216*	1.884*	1250*
Heat pad layer	1.6e-15†	7†	0.216*	1.884*	1250*
Conducting Gel (various).	0.11 - 6.2§	(80)§			

4 RESULTS AND DISCUSSION

A selected range of simulation results related to optimizing performance of equipment for thermostimulation of muscle tissue are presented to show how a multiphysics simulation tool can aid in the design of such equipment. The first set of the simulations look into aspects related to heating of muscles, with special emphasis on body composition, heating time, heating pad layout and alternative heating methods. The second set of simulations is centered on optimization of the electrical stimulation part of the equipment. In this part body composition and electrode layout are studied. As discussed earlier, the quantitative outcome of the simulations should be used with great care as there is large uncertainty in the material properties. We have nevertheless chosen to quantify the outcome of the simulations in order to illustrate the qualitative effects of e.g. body composition and heat pad layout.

4.1 Heating of biological tissue – conventional

The main purpose of the heating part of thermostimulation equipment is to warm the muscle tissue in order to improve the effect of the electrical stimulation. When using electrical heat pads as applied in conventional thermostimulation equipment, only part of the heat applied at the skin will propagate into the muscles. The resulting temperature in the muscles, and the time it takes to heat the muscles, will be very dependent on the body composition of the subject, in particular on the fat layer thickness as fat has an isolating effect. Thus it is of interest to study the influence of body composition on the heating effect, to be able to know how well heating equipment may work for different subjects. Specific parameters of interest here are the maximum achievable temperature in the muscle tissue and the heating time required to reach the maximum temperature. The layout of the heat pad, i.e. the heat wire thickness and spacing, will also strongly influence the temperature achievable in the muscles.

The first set of simulations are designed to study how the fat layer thickness influences on the steady state temperature. The layered axisymmetric model is used for the simulations. Figure 6 shows the steady state temperature distribution in the layered model, i.e. when the heating has been applied for so long time that the heat distribution is constant, for the nominal case with a fat layer thickness of 10 mm. The slope of the temperature curve is steeper in the fat layer than in the muscle layer. This means that most of the heat is absorbed in the fat layer. The temperature increase in the muscle for the example case is only between one and two degrees from the intial value of 37 ºC, whereas the temperature increase in the outer part of the fat layer is up to nearly five degrees.

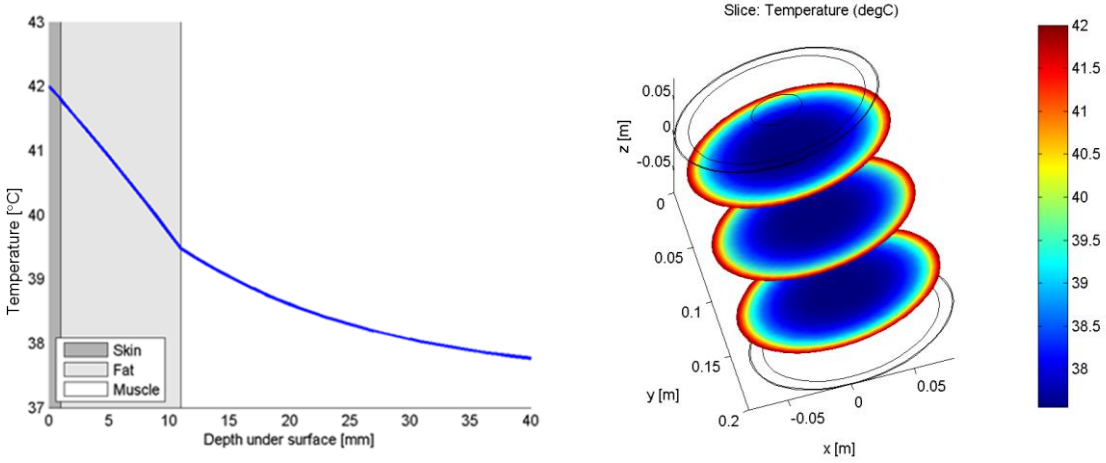

Figure 6. (a) Temperature distribution as a function of depth under surface for a fat layer thickness of 10 mm simulated using the axisymmetric model. (b) 3D representation of the temperature distribution.

When the fat layer thickness is varied, the temperature in the muscle tissue varies accordingly. Figure 7 shows the heat distribution at various positions within the muscle tissue as a function of fat layer thickness. Results are plotted for positions at the fat/muscle layer interface and for positions between 5 and 40 mm into the muscle. From Figure 7, the temperature at a given position within the muscle tissue for a given fat layer thickness may be read off. Note that values read off from Figure 7 gives a maximum value for the temperature at the given position in the muscle tissue, as a uniform heat of 42 ºC is applied at the skin for these simulations. For the real-world case of heat pads which do not cover all of the skin, the heating effect is lower as is discussed later.

It is observed that the maximal achievable temperature varies with fat layer thickness according to a curve with exponential characteristics. Thus, high muscle temperatures can only be obtained for thin fat layers. According to the simulations, a temperature increase of more than four degrees at the fat/muscle layer interface can be achieved if the fat layer thickness is below 1 mm - whereas this temperature increase is only around 1.5 ºC for a

30 mm fat layer. A similar variation of the maximal achievable temperature is seen when going into the muscle, although the variation with fat layer thickness is less marked for positions further into the muscle. For example, considering a position 20 mm into the muscle, the maximal achievable temperature increase for a patient with 1 mm fat layer is around 1.5 ºC compared to 1 ºC for a 10 mm fat layer and down to 0.7 ºC for a 30 mm fat layer.

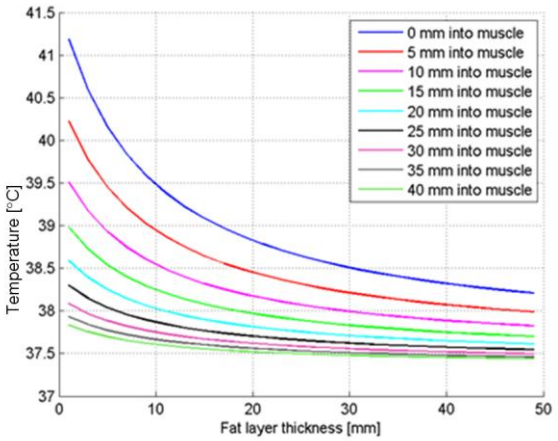

Figure 7. Temperature range inside muscle as a function of fat thickness. The upper and lower curves illustrate the temperature at the outside (close to fat) and the inside (close to the bone) of the muscle, respectively.

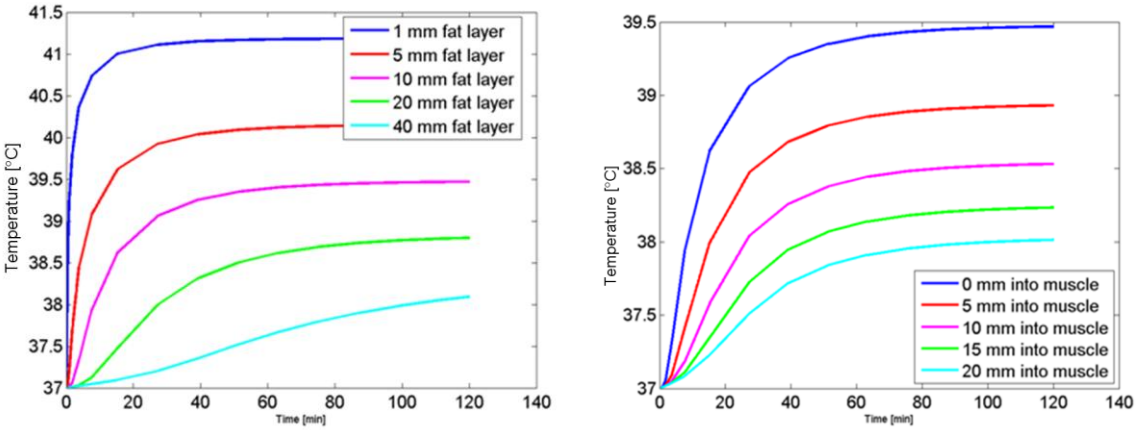

(a) (b)

Figure 8. (a) Temperature at muscle/fat layer interface as a function of time for fat thickness of 1- 40 mm. (b) Temperature as a function of time at different positions in the muscle for a fat layer thickness of 10 mm.

The effect of electrical muscle stimulation will depend on the applied current level and the treatment time. The optimal treatment time for a patient is shorter than the maximum heating time a patient can withstand. The electrical stimulation should therefore not start before a sufficient muscle temperature has been reached.The fat thickness has a strong influence on both the final muscle temperature and the time needed to get sufficient heat into the muscle. Thus, the time needed for preheating of a patient before starting muscle stimulation has to be adjusted according to the patient's fat layer thickness if a certain temperature is to be achieved in the muscle. As show in Figure 8(a) for the axisymmetric model, the heating time increases when the fat layer thickness is increased. To get a temperature increase of one degree at the fat/muscle interface for a patient with fat layer of 5 mm takes 2 minutes, while getting the same temperature at the fat/muscle interface for a patient with fat layer thickness of 20 mm takes 30 minutes and nearly 2 hours for a patient with fat layer thickness of 40 mm.

The time it takes to heat up the muscle tissue increases when going into the muscle. Figure 8(b) shows the variation in heating time at certain points within the muscle and on the muscle/fat boundary for a fat layer of 10 mm. The temperature in the tissue varies according to a curve which has exponential characteristics with time. After 20-30 minutes the temperature is around 0.5 ºC below the steady-state temperature. At the muscle/fat layer interface 72% of the temperature increase happens within the first 20 minutes and 84% of the temperature increase happens within the first 30 minutes. Considering a position 20 mm into the muscle, only 30% of the temperature increase happens within the first 20 minutes. To get 80% of the temperature increase, a heating time of 50 minutes is required. This illustrates that a longer heating time is required to obtain deep heating of the muscles.

Heat pads are generally built up from heat wires with a given spacing between the wires. This heat wire spacing leads to the heating effect being uneven, and also to a lower temperature than if uniform heat is applied at the entire skin surface. In order to study the effect of this non-uniform heating, the surface area is divided into equally sized regions with equal spacing, for which heat is applied. Comparison is done with the case for which there is uniform heating to 42 ºC at the outer edge of the skin. For all cases, a fat layer thickness of 10 mm is considered. Figure 9 shows the case with two 5 mm wide heat wires separated by 5 mm spacing, and Figure 10 shows the case with eight 1.25 mm wide heat wires separated by 1.25 mm spacing. The heating effect of the two wire case is very uneven – giving a temperature variation of more than 1.2 ºC at the fat/muscle interface. The effect is lower at deeper muscle positions, but a significant reduction of the heat compared to the uniform heating case is observed. The maximum heat loss compared to the uniform case is 1.5 ºC at the fat/muscle interface and about 1.0 ºC at a position 10 mm into the muscle. For the case with eight heat wires with heat wire width of 1.25 mm and 1.25 mm heat wire spacing (Figure 10), the maximum heat loss compared to the uniform case is only 0.4 ºC at the fat/muscle interface and 0.15 ºC at a position 10 mm into the muscle. Note that the blood temperature is assumed to be constant (37 ºC) in the simulations, and the effect of transportation of blood heated by the heat wires to regions without heat wires is therefore not included. In the current simulation series, the heat wire spacing is set equal to the heat wire width. If the heat wire width is set larger than the heat wire spacing, a more even temperature distribution can be achieved with a larger heat wire spacing.

Based on these simulations, it is evident that the heat wire spacing should be kept as low as possible in order to get a maximum heating effect in the muscle tissue. A 5 mm heat wire spacing leads to significant lowering of heat in the muscle tissue compared to the ideal case of uniform heat applied over the entire skin surface.

A simulation using a full 3D model with realistic pad size has been made in order to apply the results in the preceding sections on a more realistic case. The simulation results are shown in Figure 11. From Figure 11 it is observed that most of the muscle tissue in the example case is heated more than one degree using the two heat pads at opposite sides. As expected, the results from the axisymmetric simulations above agree well with the results from the 3D simulation model, and thus the results from the parametric studies with the axisymmetric model are valid for analysis also for the more general case. Note, however, that for each heat pad, a uniform temperature of 42 ºC is applied instead of using heat wires, i.e. this represents an overestimation of the temperature in the tissue.

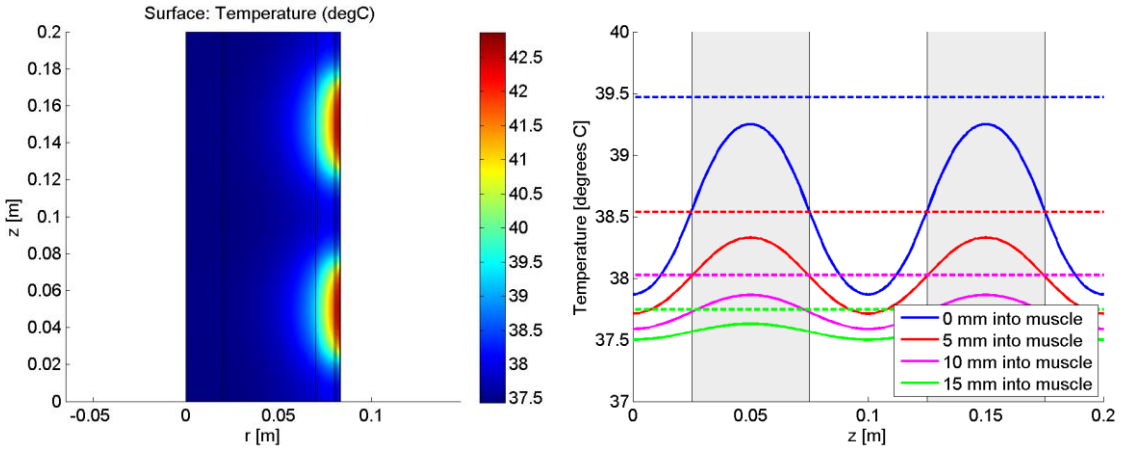

Figure 9. Heating of selected parts of the surface – 2 heat wire case corresponding to 5 mm wire separation. (a) Heat distribution shown in an axisymmetric plot. (b) Heat distribution along length of model at the fat layer/muscle layer interface and at three different positions in the muscle tissue. Compared to the uniform case

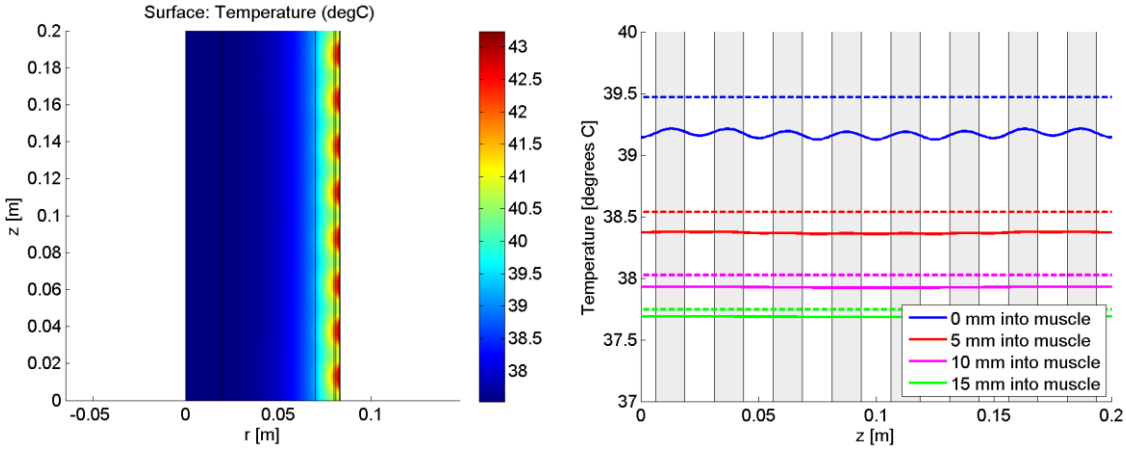

Figure 10. As Figure 9 but for the 8 heat wire case corresponding to 1.25 mm wire separation..

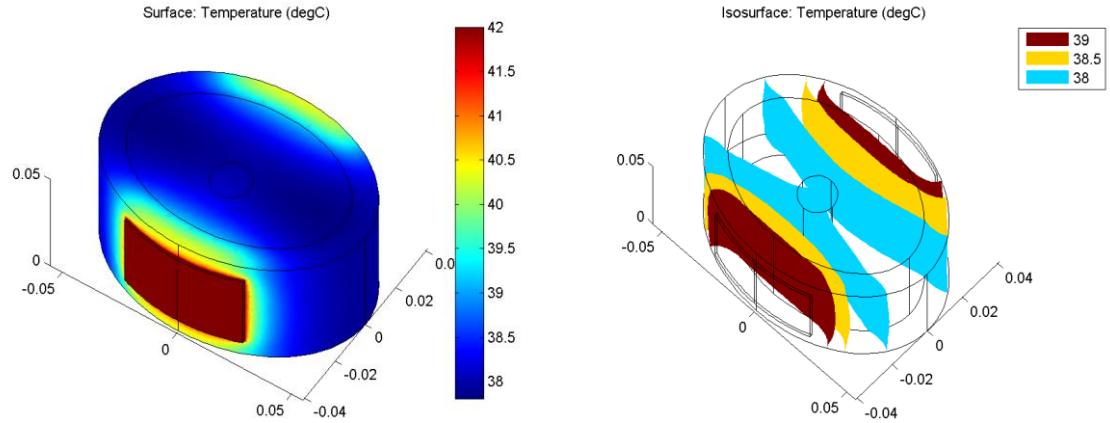

Figure 11. Results from full 3D model simulations. (a) 3D plot of temperature distribution. (c) Iso-surface plot which shows the areas within the tissue for which the temperature is 39 ºC, 38.5 ºC and 38 ºC.

4.2 Heating of biological tissue – comparison of conventional with microwave and IR

As shown in previous section, the heating effect in the muscles when using conventional heat pads is rather modest. In the following, the heating effect of infrared and microwave heating is compared to conventional heating.

The simplified axisymmetric layered model is used to model the effect of infrared heating. Figure 12(a) shows a comparison between IR heating and heating using heat pads. Only a slightly higher temperature (approximately 0.2°C) is obtained at the fat-muscle boundary when using IR heating. The simulations confirm that the most of the absorption of IR radiation occurs in the skin layer, and that the heat is transferred to deeper tissues by heat conduction. Thus, this confirms that IR radiation does not give a deep heating of muscle tissues and that rather long treatment time is required for the heat to reach steady state as in the case with conventional heating using heat wires.

Figure 12(b) shows the heat distribution generated by microwave radiation, and the much deeper penetration of microwaves than infrared is clearly observed. Microwave energy can either be applied directly to the skin without any cooling (blue line; corresponding to the cases with infrared heating and conventional heating in Figure 12(a)), or with additional cooling of the skin using e.g. a bolus with deionized water (red line). With the skin-cooling method the required therapeutic temperature can be reached without the risk of overheating the skin. However, it is difficult to control the actual temperature inside the muscles as no practical non-invasive temperature measurement methods exist, and thermal simulations can not give exact predications of temperature. It may therefore be safer to apply the method without skin cooling, as temperature sensors placed on the skin surface can be used for temperature control. The simulations indicate that a temperature around 40 ºC can be obtained a couple of cm into the muscles without skin cooling, which is higher than the maximum temperature at the fat/muscle interface reached with conventional or IR heating.

4.3 Stimulation of tissue using electric fields

A set of COMSOL Multiphysics models have been made in order to simulate how the electrical stimulation effect in thermostimulation equipment is influenced by design choices. The first part of this section looks into how to design the electrodes in order to achieve uniform excitation of a muscle. The second part looks into the effect of gel leakage on the stimulation effect.

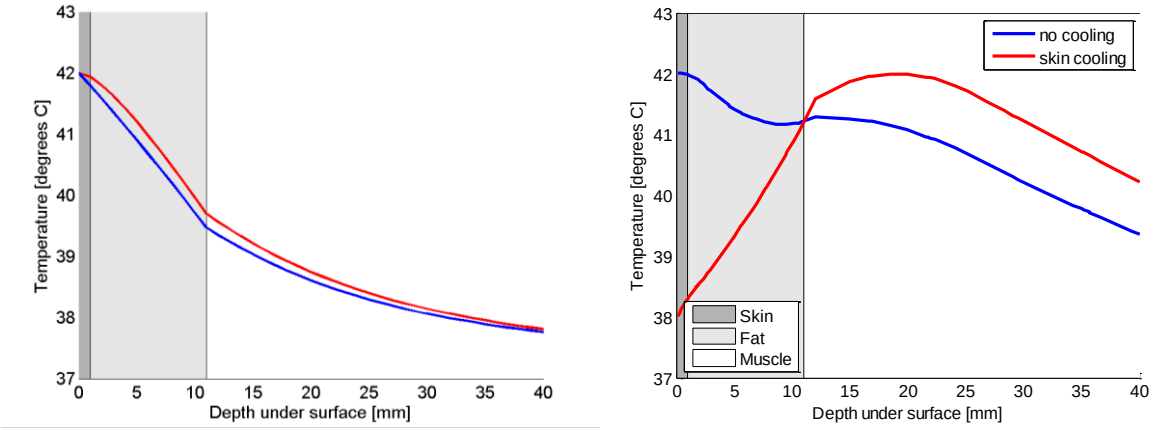

(a) (b)

Figure 12 (a) Temperature distribution using infrared heating (red) compared to heating using heat pads (blue). The biological properties given in Table 1 are used in the simulations. (b) Temperature distribution when heating with microwaves. The red line is for microwaves applied directly on the skin without cooling whereas the blue line is when the skin is cooled to 38°C using e.g. deionized water. The biological properties given in Table 1 are used in the simulations.

In most cases it is of interest to optimize thermostimulation equipment to stimulate uniformly in the muscle below the electrodes. If the electric field is non-uniform, the electric field may be above the critical electric field which gives stimulation only in parts of the muscle for a given electrode stimulation current. Due to the pain threshold of the patient, the stimulation current cannot be increased, and thus one can risk that stimulation will only occur at one end of the muscle, or alternatively that the stimulation goes deeper into the muscle in one part of the muscle than on the other part.

To achieve uniform electric field and electric current in the muscle, the electric field which is set up should thus be uniform along the length of the muscle. On the other hand, low electrode conductivity is requested in order to have a soft and bendable stimulation pad. When the electrode conductivity is low, the electric potential will in the general case vary significantly along the electrode, especially if the contact points for the electrodes are at the same edge of the electrodes. One question asked during the design of stimulation pads was how low the electrode conductivity could be while still having uniform stimulation in the muscles if the contact points were on the same edge of the electrodes. It was also of interest to find out how the situation changes with contact points at opposite edges of the electrodes, and to what extent it would help to have a thin conductor with high electric conductivity under the electrodes. To answer these design questions, simulations were done using a 3D layered model.

In Figure 13 the case with low electrode conductivity of 0.1 S/m is considered. This gives a soft and bendable stimulation pad which is ideal seen from the usability side. Two different cases with respect to contact point are compared; contact points at the same edge shown in Figure 13(a) and (c), and at opposite edges show in Figure 13(b) and (d). From the figures it is evident that the potential difference laterally between the electrodes varies significantly for the case with contact points at the same edge – from 10 V at one edge of the electrodes and down to 1 V at the other edge. For the case with contact points on opposite edges, the variation in potential difference laterally between the electrodes is much lower The maximum potential difference is around 5 V close to the edges and down to around 2 V towards the middle of the electrodes.

In Figure 14 the electric field in the muscle tissue is compared for the two cases of contact points on the same side of the electrodes and contact points on opposite sides of the electrodes. From the figure it is evident that the electric field in the muscle is very non-uniform for the case with contact points on the same sides of the electrodes, as to be expected based on the potential difference on the electrodes. Placing the contact points on opposite sides reduces the non-uniformity, but a uniform field distribution in the muscle tissue is still not obtained.

From the above considerations, it is clear that having contact points on the same side of the electrodes and electrode conductivity as low as 0.1 S/m is not a good design choice for the stimulation electrodes. It was therefore of interest to investigate how low electrode conductivity would give acceptable uniformity of the electric field in the muscles when using contact points at the same edge of the electrodes.

To investigate the effect of electrode conductivity, simulations with varying parameters for the conductivity of the electrode were done. Simulations were done for conductivities ranging from 1 MS/m (metal) to 0.1 S/m (poor conductor). Figure 15 shows how the electric field in the tissue varies with electrode conductivity for four selected electrode conductivities, 1 MS/m, 40 S/m, 10 S/m, and 0.1 S/m. It is evident that a significant degree of non-uniformity is introduced in the electric field in the muscle when decreasing the conductivity in the electrodes. To make a more quantitative assessment of the influence of the electrode conductivity on the electric field distribution in the muscle, the electric field is evaluated along a line in the muscle tissue parallel to the electrodes (denoted “line A”, see Figure 5). The electric field evaluated along line A for 7 different electrode conductivities is shown in Figure 16(a). From the figure it is seen that when the conductivity decreases, the electric field is focused in a small region close to one end of the electrode. This gives very low values of electric field at the other end of the electrode, leading to difficulties in achieving the “critical electrical field” for stimulation in this part of the muscle while being below the pain threshold of the patient.

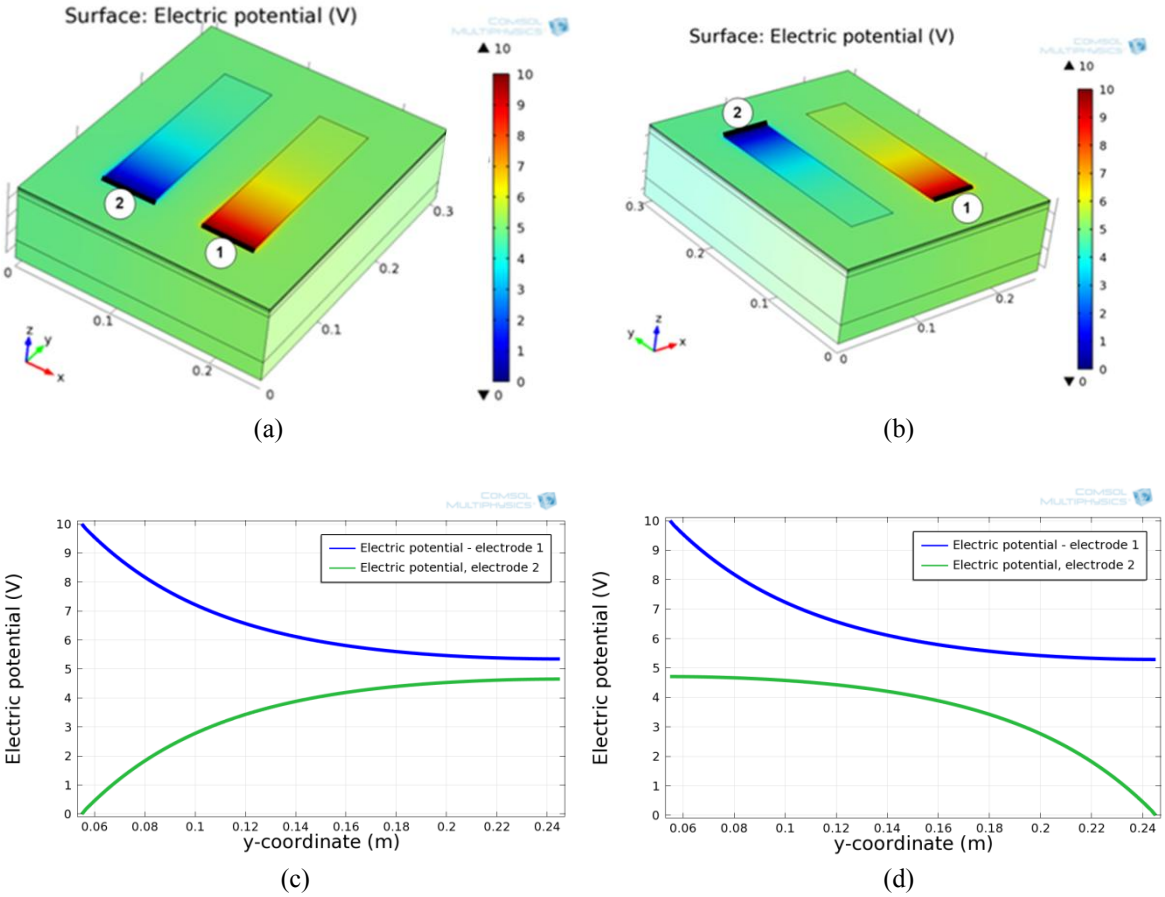

Figure 13. Comparison of contact points on the same edge and contact points on opposite edges for electrodes with conductivity 0.1 S/m. (a),(c): Contact points on the same edge. (b),(d): Contact points on opposite edges.

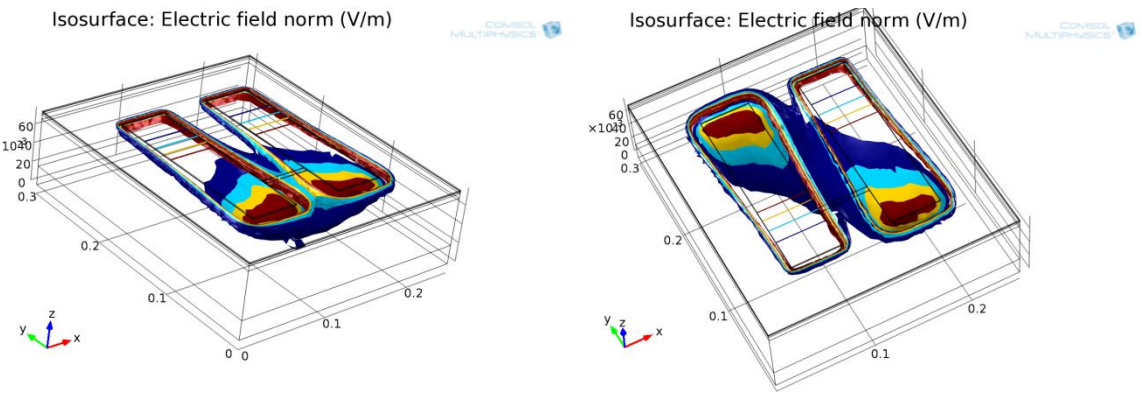

Figure 14. Electric field in the muscle compared for different contact points for electrodes with conductivity 0.1 S/m.

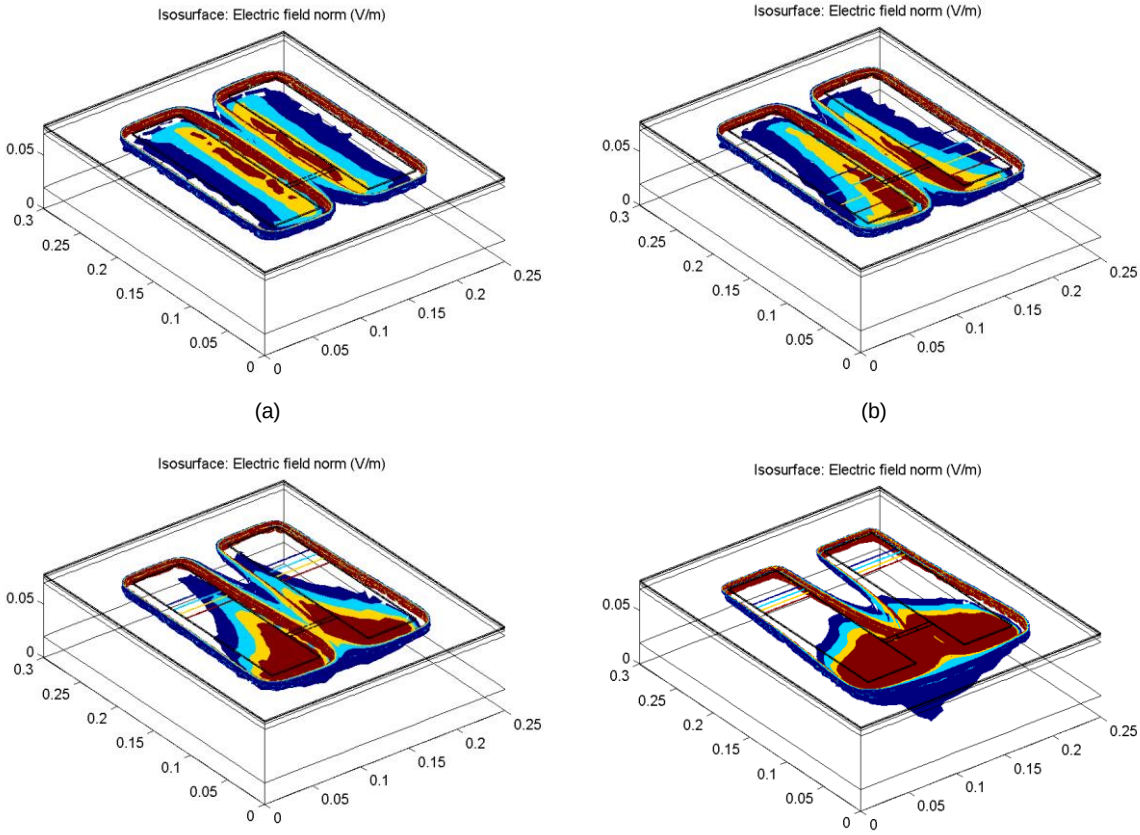

Figure 15. 3D isosurface plot of the electric field in the tissue with varying electrode conductivity. Isosurfaces are plotted for electric field values of 10 V/m, 12 V/m, 14 V/m and 16 V/m. (a) Electrode conductivity of 1 MS/m (b) 40 S/m (c) 10 S/m (d) 0.1 S/m

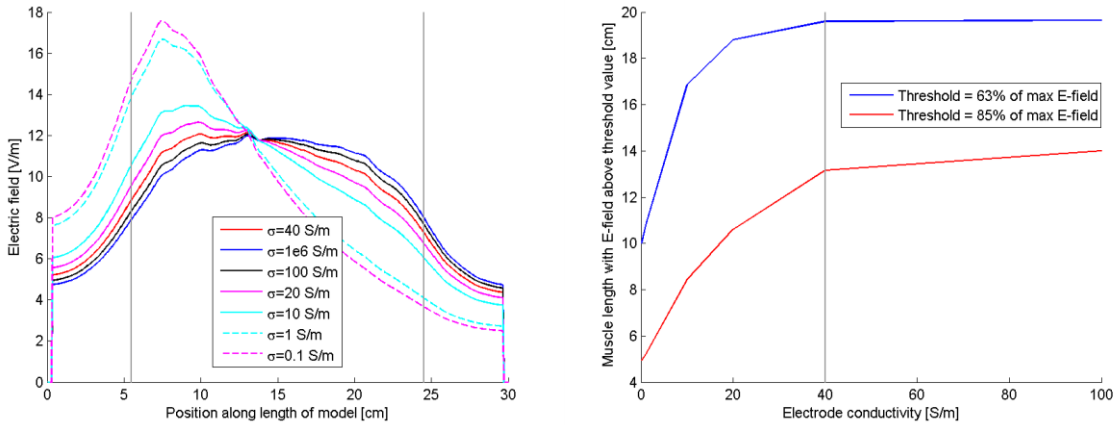

Figure 16. (a) Electric field evaluated along line A for variation in electrode conductivity.(b) Length of muscle where the the electric field is above a 63% and 85% of the maximum electric field as a function of electrode conductivity (corresponding to the width of the peaks in (a)). The electrode length is 19 cm.

In Figure 16(b) the results are summarized by plotting the length of the muscle for which the electric field is above a certain percentage of the maximum value as a function of electrode conductivity. Looking at the curve for 63% of the maximum electric field, it may be observed that for electrode conductivities above 40 S/m the electric field is above 63% of the maximum value for all of the length directly under the electrodes, i.e. 19 cm. Going down to an electrode conductivity of 10 S/m reduces the length to 17 cm, and going further down to an electrode conductivity of 1 S/m reduces the length to around 10 cm. Similar results are seen for the 85% case, where the length for which the electric field is above 85% of the maximum value is reduced from around 14 cm for 40 S/m to 5 cm for 1 S/m. As a conclusion from these simulations, it is recommended to use an electrode conductivity higher than 40 S/m - especially if two contact points at the same end of the electrodes is used.

A method to compensate for poor electrode conductivity is to integrate a wire with high conductivity under the electrodes. This introduces some challenges related to production of the electrodes, but it was still found interesting to see how this affects the electric field distribution. This scenario was simulated using the model shown in Figure 5 (b). The shape of the wires was chosen in order to investigate a worst-case situation in which the distance between the wires with high conductivity is large at one end of the electrodes and small at the other end of the electrodes. This is illustrated in Figure 17 and Figure 18. Here only two electrode conductivities are considered – the metal case with conductivity of 1 MS/m and the case with a very poor conductivity of 10 µS/m. In Figure 18 a range of electrode conductivities between 10 µS/m and 1 MS/m are considered. From the figures it is evident that when a conductive wire is used below the electrodes, there is no significant variation in stimulation along the electrode, even if very poor electrode conductivity of 10 µS/m is used.

In Figure 19 the variation in current density and electric potential over the electrodes is plotted. Observe the high current density around the wires. Here the wire acts as a narrow electrode, and the poor electrode conductivity in the electrode may therefore lead to localized high currents. The effects of these high currents should be further investigated. Due to the high current density, it is recommended to keep the electrode conductivity above 1 S/m if the effects of higher current density on heat generation are not investigated.

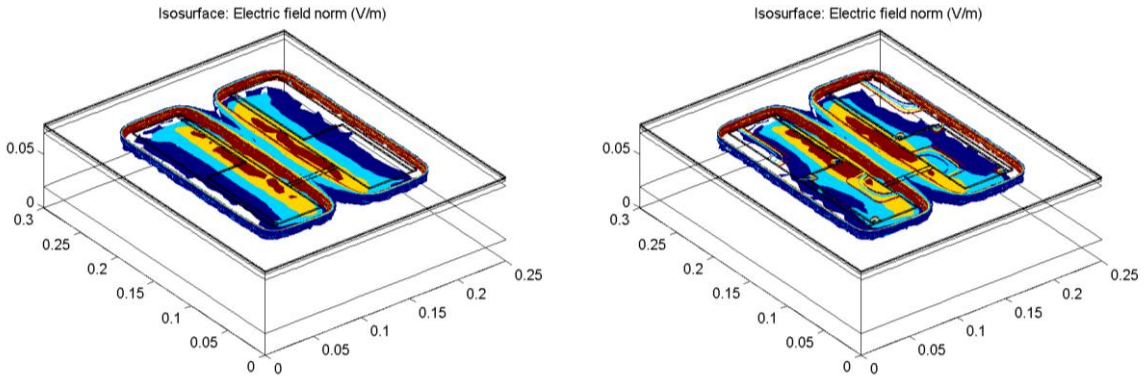

(a) (b)

Figure 17. Conductive electrodes with wire. 3D isosurface plot of the electric field in the tissue with varying electrode conductivity. Isosurfaces are plotted for electric field values of 10 V/m, 12 V/m, 14 V/m and 16 V/m. (a) Electrode conductivity of 1 MS/m (b) 10 µS/m.

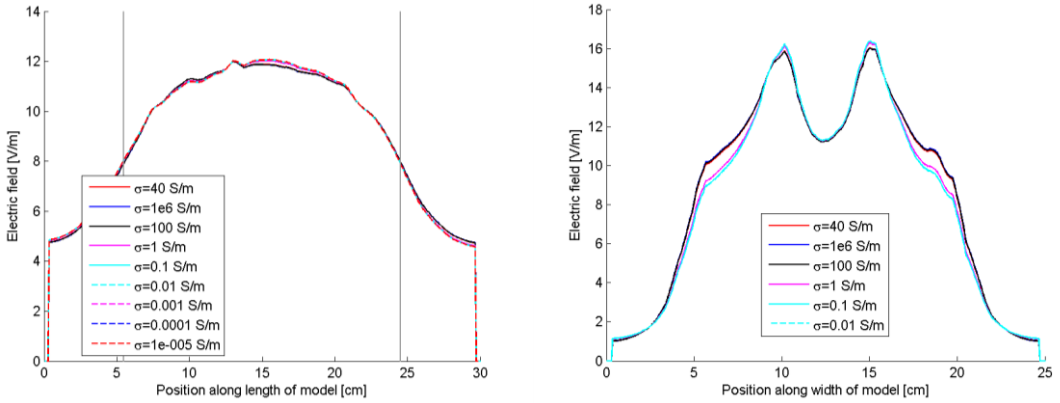

(a) (b)

Figure 18. Conductive electrodes with wire. (a) Electric field along Line A parallel to the electrodes in the muscle tissue [cf. Figure 5 (b)]. (b) Electric field along Line B perpendicular to the electrodes.

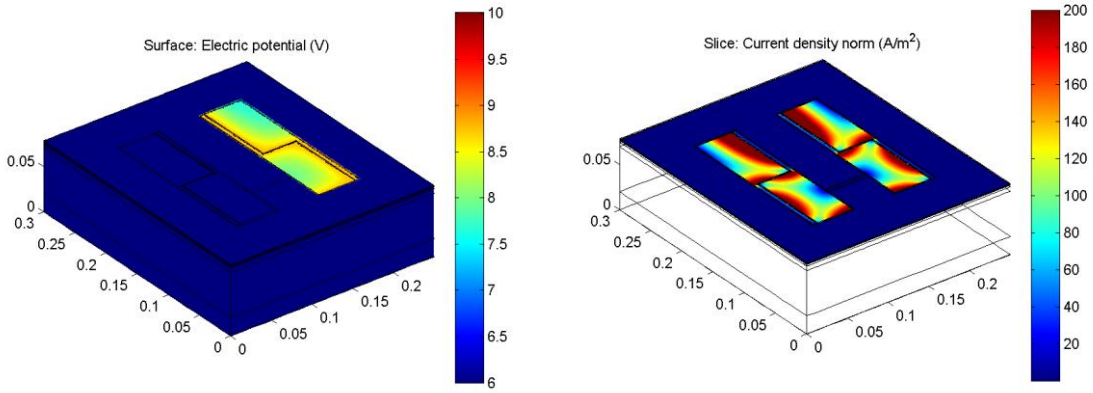

(a) (b)

Figure 19. Conductive electrodes with wire. (a) Electric potential and (b) current density in the electrodes for the case of very poor electrode conductivity of 10 µS/m.

4.4 Use of conductive gel under stimulation electrode

A film of conductive gel is typically applied under the electrodes in order to secure good electrical contact between the electrodes and the skin. Simulations were performed to investigate the effect leakage of gel from the electrode area to the gap between the electrodes. This is done by including a strip of gel which covers part of the gap between the electrodes, as shown in Figure 5 (b).

The amount of gel spillage is varied by varying the length of the area for which there is leakage (from 2 mm to 30 mm) and the gap between the two parts of the gel leakage (from 4% of the length between the electrodes covered with gel to all of the length between the electrodes covered with gel). In the simulations it is assumed that the gel leakage is symmetric around the centreline between the electrodes. For all the gel leakage simulations, an electrode conductivity of 40 S/m is assumed. The conductivity of the gel is set to be 6.2 S/m for all simulation except for the results presented in Figure 25 for which the conductivity is set to 0.11 S/m.

This work does not look into the heating effect introduced by increased current density below the electrode due to areas without gel under the electrodes. Several literature results (see e.g. Nelson 1999) indicate that this heating effect may be problematic – in some cases even lead to pain and burns – if the gel is not evenly applied.

Figure 20 shows the electric field in the tissue and the current density in the gel plane for varying widths of gel spillage for the case of 30 mm gel leakage length. From the figure it is evident that the gel leakage has significant influence on the electric field in the tissue for the 40% and 80% gel leakage cases. This is studied in more detail in Figure 21(a), where the electric field along the length of the model 1 mm into the muscle is studied for varying gel width. A significant focusing of the electric field is seen already from gel widths of 20% of the gap between the electrodes, going up to very high values for a gel width of 80% of the gap. In Figure 22 a shorter strip of gel leakage (2 mm long) is considered. For this case, the focusing effect of the electric field is much less visible.

Figure 23 summarizes the most important results from Figure 21 and Figure 22, showing how the gel leakage width, length and thickness influence on the length of the muscle for which the electric field is above 63% of the maximum value of the electric field. It is observed that both the length and the width of the gel strip influence significantly on the electric field through focusing of the electric field in the area below the gel strip, whereas the gel thickness does not influence the electric field in the muscle significantly.

The final case considered is the case where the gel leakage creates contact between the electrodes, e.g. gel leakage width of 100%. Simulation results for this case are shown in Figure 24. It is evident that contact between the gel between the electrodes leads to more of the current between the electrodes going directly in the gel instead of going through the tissue, thus reducing the electric field in the muscles significantly. The resultant electric field in the muscles is more focused than in the case without gel, but on the other hand, the electric field distribution in the muscle is more uniform than for the case with 80% gel leakage. However, the contact between the gel leakage from both electrodes leads to localized very high currents in the gel. The effects of these high currents – and the potential for giving burns based on these currents - should be further investigated.

All results presented so far have been for a gel conductivity of 6.2 S/m. In Figure 25 it is investigated how using a gel with poor electrical conductivity of 0.11 S/m influences on the stimulation along the muscle. As expected, the use of a gel with poorer conductivity leads to more even stimulation along the length of the muscle for a given area of gel leakage. The challenge when using a low conductivity gel is the heating effect introduced by increased current density due to areas under the electrodes without gel. This effect has not been studied in detail in the present work, but may be a topic for further work.

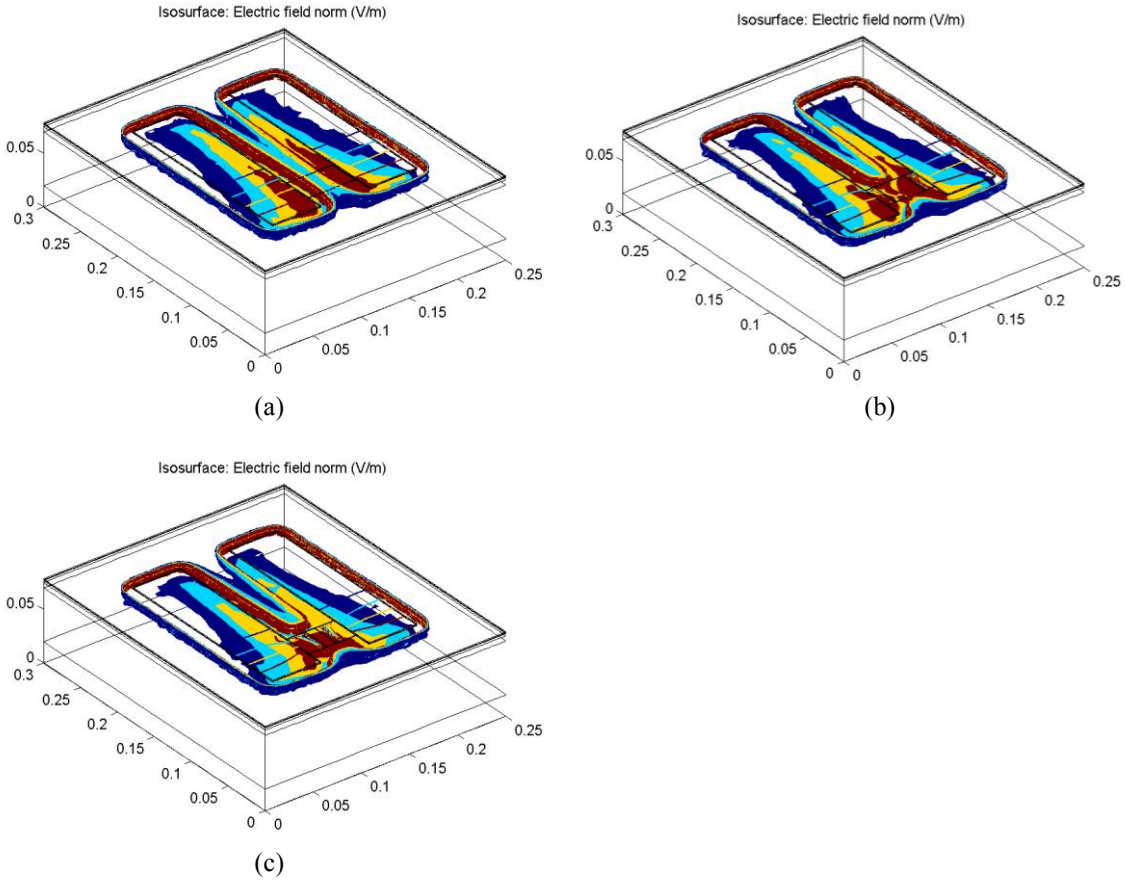

Figure 20. Electric field in the tissue for length of gel spillage of 30 mm and width of gel spillage of 4% of gap between electrodes (a), 40% (b) and 80% (c).

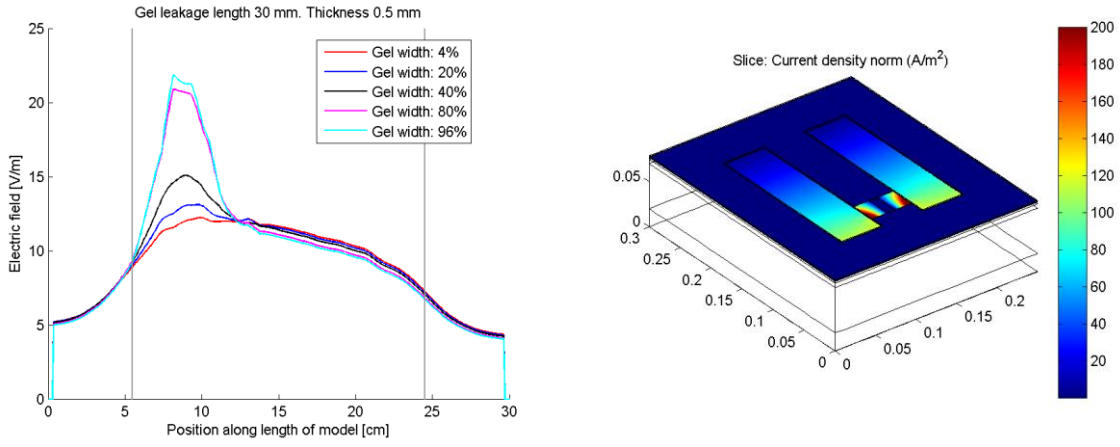

Figure 21. (a) Variation of electric field with gap width evaluated along line A for a gel leakage length of 30 mm and gel thickness of 0.5 mm, (b) Current density for the case with gap width of 80%.

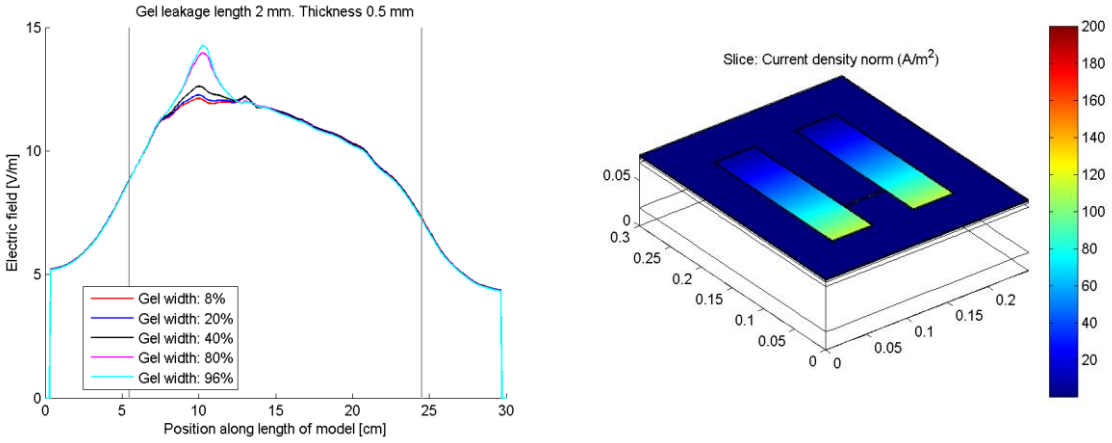

(a) (b)

Figure 22. As Figure 21, but for gel leakage length of 2 mm and gel thickness of 0.5 mm

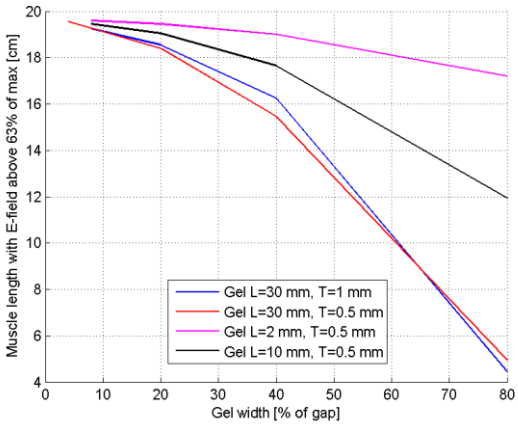

Figure 23. Muscle length for which electric field is above 63% of maximum value of electric field as a function of gel leakage width for different gel leakage lengths and thicknesses.

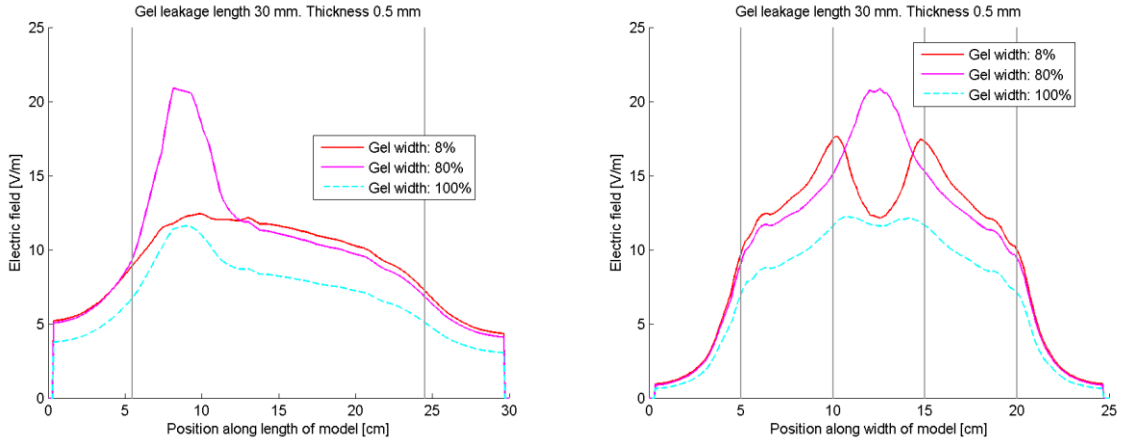

(a) (b)

Figure 24. Gel leakage across (a) the length of the model corresponding to line A in Figure 5 (b) and (b) the width of the model corresponding to line B in Figure 5 (b) for varying gel leakage widths between 8% and 100% of the distance between the electrodes. Gel leakage length is 30 mm and gel thickness is 0.5 mm for all cases. Gel conductivity is 6.2 S/m.

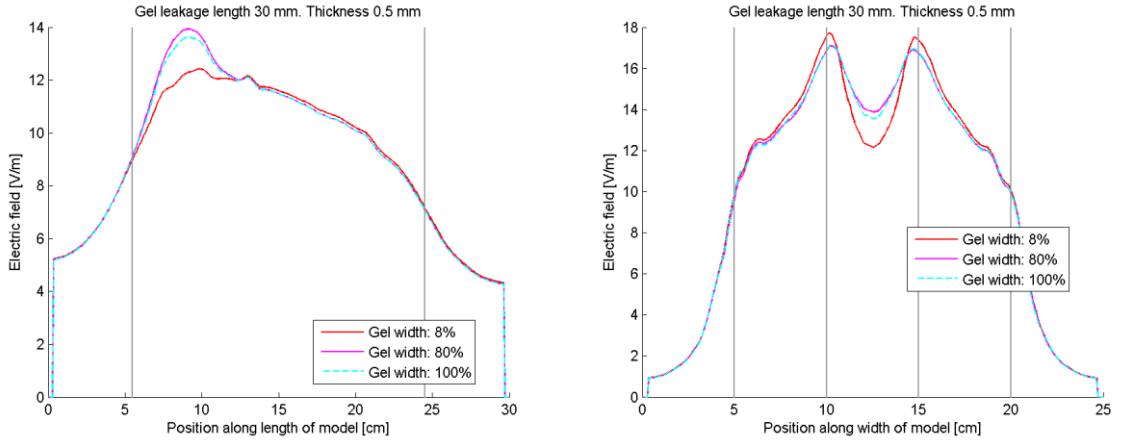

(a) (b)

Figure 25. As Figure 24, but for gel conductivity of 0.11 S/m.

5 Summary and Conclusions

The present work has illustrated how a multiphysics simulation approach can be used in order to model medical equipment. The finite element package COMSOL Multiphysics was used for the simulations. It was shown that important qualitative conclusions can be drawn from the multiphysics simulations, and that the multiphysics approach is an important aid when designing thermostimulation equipment. However, the results must be used with care as there are large uncertainties in the simulated values reported due to the simplified modelling and the large variations in the properties of the biological materials found in literature. More accurate knowledge of electrical and biological tissue properties and their temperature dependency would encourage simulating the effects of combined heating and electrical stimulation.

From the simulations of conventional heat pads it was found that the temperature in the muscles varies with fat layer thickness according to a curve with exponential characteristics. The fat layer thickness has a strong influence on both the final muscle temperature and the time needed to get sufficient heat into the muscle. Thus,

the time needed for preheating of a patient before starting muscle stimulation has to be adjusted according to the patient's fat layer thickness if a certain temperature is to be achieved in the muscle. It was also found that the heat wire separation is a critical parameter which influences strongly on the uniformity of the temperature distribution along the length of the muscle.

Simulations verified that the thermal effect of infrared heating and heat pads are comparable, but neither of the techniques can give deep heating of muscles. Microwave heating gives a direct heating of the muscles and a higher temperature can therefore be achieved. Also steady state temperature is reached faster when using microwave heating than conventional heating or infrared heating.

The second part of the paper considered electrical stimulation of muscles. It was shown that the conductivity of the stimulation electrodes has significant effect on the distribution of the electric field within the muscles. Due to the pain threshold of the patient, the stimulation current cannot be increased, and therefore low electrode conductivity can lead to one end of the muscle being stimulated whereas the other end of the muscle is not being stimulated, or that the stimulation does not reach deep into the muscle. From the simulations in this work it is recommended to use an electrode conductivity of 40 S/m or higher if two contact points at the same end of the electrodes is used for application of the stimulation current. These simulations are made for an electrode length of 19 cm. For longer electrodes, even higher electrode conductivity should be used if using only two contact points at the same end of the electrodes. By using diagonal contact points one may get acceptable performance also with somewhat lower electrode conductivity.

If a wire or foil with high conductivity is introduced below the electrode along all of the electrode length, the electrode conductivity is not critical with respect to the uniformity of the electric field in the muscle. Note, however, that when a wire is used, very poor electrode conductivity may lead to localized high currents – the effects of these high currents should be further investigated.

Leakage of conductive gel from the electrode area leads to focusing of the electric field in certain regions. The amount of focusing depends on the amount of gel leakage. In general all gel leakage outside the electrodes should be avoided. As for the low electrode conductivity, this can lead to one area of the muscle (the part where there is gel leakage) being stimulated, whereas the other parts of the muscle are not stimulated. Great care during gel application, and gel application at the electrode surfaces rather than at the skin is required in order to minimize the effect of gel leakage.

REFERENCES

Bjordal, J. M., Johnson, M. I. and Christian Couppè. (2001). *Clinical electrotherapy: your guide to optimal treatment*. HøyskoleForlaget.

Bronzino, J. D. (2000). The biomedical engineering handbook, Springer.

Carrara N, (2010). Dielectric Properties of Body Tissues: Webpage: http://niremf.ifac.cnr.it/tissprop/.

Datta, A., and Rakesh, V. (2009) An Introduction to Modeling of Transport Processes: Applications to Biomedical Systems. Cambridge University Press,

Drizdal, T., Togni, P., Visek,L. and Vrba, J. (2010). Comparison of Constant and Temperature Dependent Blood Perfusion in Temperature Prediction for Superficial Hyperthermia. *Radioengineering* 19, no. 2: 281.

Duck, F.A., (1990). Physical properties of tissue: a comprehensive reference book, Academic Pr.

Fiala, D., Lomas, K.J. & Stohrer, M., (1999). A computer model of human thermoregulation for a wide range of environmental conditions: the passive system. *J Appl Physiol*, 87(5), 1957-1972.

Filipovic, N.D. et al., (2011). Transient finite element modeling of functional electrical stimulation. General physiology and biophysics, 30(1), p.59.

Giombini, A., Giovannini, V., Di Cesare, A., Pacetti, P., Ichinoseki-Sekine, N, Shiraishi, M., Naito, H. and Maffulli, N. (2007) Hyperthermia induced by microwave diathermy in the management of muscle and tendon injuries. *British Medical Bulletin* 83, no. 1: 379 -396.

Habash, R. W. Y., Bansal, R., Krewski, D. and Alhafid, H. T. (2006) Thermal therapy, part 2: hyperthermia techniques. *Critical Reviews in Biomedical Engineering* 34, no. 6: 491-542.

ICNIRP, (2006) *ICNIRP statement on far infrared radiation exposure*, Health Physics 91, no. 6: 630-645

Kreith, F. and Goswami, D. Y., (2005). *The CRC handbook of mechanical engineering*, CRC Press.

Kuhn, A., and Keller, T. (1999) 3D transient model for transcutaneous functional electrical stimulation. In International functional electrical stimulation society conference, page 385–387.

Matweb, (2010), Webpage: Summary of similar materials in the MatWeb database for the category "Silicone Rubber", accessed October 28th 2010. http://www.matweb.com/search/DataSheet.aspx?MatGUID=cbe7a469897a47eda563816c86a73520

Mohammed, Y. and Verhey, J., (2005). A finite element method model to simulate laser interstitial thermo therapy in anatomical inhomogeneous regions. *BioMedical Engineering OnLine*, 4, no 1: 2

Mortimer, J. T, and Bhadra, N. (2004). Peripheral nerve and muscle stimulation. in Neuroprosthetics: theory and practice. Singapore: World Scientific Piblication Co Inc. Editors: Horch KW and Dhillon GS.

Nelson, R. M., Currier, D. P. and Hayes, K. W. (1999). Clinical Electrotherapy. 3rd ed. Appleton &Lange,

Pennes, H. H., (1948). Analysis of tissue and arterial blood temperatures in the resting human forearm. *Journal of Applied Physiology*, 1(2), 93.

Primasil Silicones Ltd Data Sheet, (2010). Heat Cured Conductive Silicone Rubber (HCR), Type PR 610 / 60.

Reichel, M., Mayr W. and Rattay F. (1999). Computer Simulation of Field Distribution and Excitation of Denervated Muscle Fibers Caused by Surface Electrodes. Artificial Organs 23, no. 5: 453-456.

Watlow (2010). Watlow Application Guide, Reference Data, Physical Properties of Solids, Liquids and Gases, Available from http://www.watlow.com/reference/files/nonmetallic.pdf, Accessed September 2010

Ward, A. R. (1984), Electrode Coupling Media for Transcutaneous Etectrical Nerve Stimulation, Australien J Physiotherapy, 30, 3:82-85